JOURNAL OF THERMOPHYSICS AND HEAT TRANSFER
Vol. 10, No. 2, April–June 1996

# Maximum Entropy Analysis of Chemical Reaction Energy Dependence

Michael A. Gallis* and John K. Harvey†
*Imperial College of Science, Technology, and Medicine, London SW7 2BY, England, United Kingdom*

**In this article the energy dependence of chemical and ionic reactions is examined and a new model is developed for the calculation of reaction probability and postreaction energy disposal for exchange reactions. The new model is based on the principles of the maximum entropy method. For the exchange reactions the reaction probability is based on either the translational or the vibrational energy of the reagents as appropriate, whereas for dissociation the vibrational energy is used as the controlling factor. The new method is compared with other methods used for direct simulation Monte Carlo calculations. Examples of flowfield solutions are presented and the differences between the results of the new method, those using Bird's method, and continuum solvers are discussed and evaluated.**

## I. Introduction

DURING atmospheric re-entry of spacecraft, the high temperatures that are found in the hypersonic shock layers provoke the onset of zones of chemical activity that have a very significant impact on the energy content of the flow, and hence the heat and momentum transfer to the surface of the vehicle, and the thermal radiation. Since most of the reactions absorb energy, they lessen the effects of the high-temperature flow, provided that the spacecraft's surface is non- or only partially catalytic. Reliable estimates of the heat transfer are of paramount importance to the mission designers, and are dependent on predicting accurately the flowfield associated with the vehicle, including real-gas effects and chemistry.

Usually the first type of reaction to take place is dissociation. This depletes (partially or even completely) the molecular species of the flow and the resulting appearance of atomic species is followed by a different set of chemical reactions, the exchange or shuffle reactions. These lead to further changes in the composition of the flow compared with the ambient fluid. The importance of the vibrational energy in promoting chemical reactions has been long recognized[1,4]; although dissociation reactions that are controlled by this mode dominate the chemical activity in hypersonic flows, the exchange reactions fall within a group that is influenced predominantly by the translational energy, with some exceptions that happen to be controlled by the vibrational energy. Because of their smaller energy requirements, these exchange reactions can play a decisive role in intermediate energy reacting flows, e.g., those in the 3 km/s range.

The aim of this article is to present a chemistry method for use with the direct simulation Monte Carlo (DSMC) method that recognizes the dependence of each particular reaction on the appropriate energy mode, and to include, where appropriate, the translational energy as a driving factor for exchange reactions, providing therefore a more realistic simulation of the phenomena of chemical activity in rarefied hypersonic flows.

## II. Energy Requirements of Chemical Reactions

The activation energy has traditionally been used as a measure of the energy threshold for a chemical reaction to take place when the reagents are in thermodynamic equilibrium. This criterion fails for cases when the reagents are not in thermal equilibrium. In these circumstances we have to weigh separately the significance of each energy mode in promoting a chemical reaction. In general, all available energy modes can play a role in provoking a reaction. The reaction probability $P_r$ at a collision energy $E = \Sigma E_i$, where $i$ are all of the available energy modes in a collision, is thus,

$$P_r = S_f P(E_{\text{vib}}, E_{\text{rot}}, E_{\text{trans}}, E_{\text{elec}}) \tag{1}$$

where $S_f$ is the steric factor that takes into account the effect of the orientation of the particles and $P$ is the probability of the energy modes causing a reaction. The subscripts vib, rot, trans, and elec refer to the vibrational, rotational, translational, and electronic modes, respectively.

The role of various energy modes in promoting chemical reactions at a microscopic level is not a trivial topic and a detailed review of this phenomenon is not within the scope of this article. The reader is referred to the relevant literature[1,4] where ample theoretical and experimental information is available. For the purpose of this study and to simplify the calculation of the reaction probability, we will assume the idealized situation where the reaction is controlled by one mode only, i.e., where $P_r(E) = P(E_i)$, where $i$ is the most significant of the available energy modes. It should be emphasized that this assumption has been made here to simplify the calculations and it is not a necessary condition of the method presented.

The phenomena of specificity in postcollision energy reallocation and selectivity in energy consumption promoting a chemical reaction are closely linked. It is witnessed in every reaction as a result of satisfying the principle of microscopic reversibility (or detailed balance under conditions of equilibrium). If in the redistribution of energy, a reaction favors some energy states of a particular energy mode, then the reverse reaction will proceed with greater efficiency if the energy is in that state rather than any other. An example of this phenomenon is seen in the dissociation and recombination reactions. It is well known that the greater the vibrational energy of the reagents, the more likely dissociation reactions are to take place. When the reverse recombination reaction takes place, the vibrational mode is preferentially populated, satisfying the balance of energy in equilibrium. Violation of this coupling for an equilibrium gas would lead to a continuous transfer of energy from the vibrational mode to the other modes and equilibrium would not be maintained.

The principle of microscopic reversibility can be used for the calculation of the probability of chemical reactions. This

---

Received Feb. 20, 1995; revision received July 12, 1995; accepted for publication Dec. 7, 1995.

*Research Associate, Department of Aeronautics. Member AIAA.

‡Professor of Gas Dynamics, Department of Aeronautics. Associate Fellow AIAA.

principle[1] requires that the same measure that describes the specificity in the energy disposal of the forward reaction describes the energy selectivity of the reverse reaction. Using this principle, the maximum entropy (ME) analysis for the postcollision energy states given in the following section can be repeated for the reacting energy states to formulate the chemical reaction probabilities. This means that the same formula that is used for the energy disposal can be used for the prediction of the probability of a chemical reaction.

## III. Maximum Entropy Method

In this study a new ME method is used for the simulation of chemical reactions and energy exchange. The principles of maximum entropy for the prediction of chemical reactivity were first used by Levine and Bernstein.[1] This method avoids using the equilibrium distributions that have been the basis of the DSMC algorithm of Bird[3] for the calculation of the postcollision energy exchange and chemical reaction probability. Instead, it specifies the distributions from which the post collision properties are determined by quantifying the deviations of these from the equilibrium distributions.[2] This makes the method particularly useful for the simulation of flows where significant degrees on nonequilibrium are experienced, or where features of the flow depend on nonequilibrium effects, for example, in chemical lasers.

The equilibrium distributions that are used as the starting point for analysis have been formed by Hass et al.[5] in a very compact and convenient way as

$$P(f_a) = \frac{\Gamma(\Xi_a + \Xi_b)}{\Gamma(\Xi_a)\Gamma(\Xi_b)} (f_a)^{\Xi_a - 1}(1 - f_a)^{\Xi_b - 1} \tag{2}$$

where $f_a$ is the fraction of the collision energy in mode $a$; $\Xi_a$ is the number of the degrees of freedom corresponding to the energy mode $a$, which can be the vibrational, rotational or translational mode or any combination of them; $\Xi_b$ is the total of the remaining degrees of freedom (Ref. 3); and $\Gamma$ is the gamma function.

The equilibrium energy distributions are the ones that are statistically the most likely to be realized in a gas. However, there is abundant experimental evidence[1] that these distributions are not realized in the nascent products of almost all chemical reactions. The equilibrium distributions should only legitimately be used to describe the observed distributions of the reaction products energy states as an approximation in a near-equilibrium regime. Since DSMC is usually employed for flows where this is far from the case, this assumption cannot be sustained.

In the ME formulation, the most probable distribution to be realized after a chemical reaction is calculated by estimating its departure from the corresponding equilibrium distributions, or so-called prior distribution $P^0$. To calculate the most probable distributions based on the information the prior distributions give us about the system, we need an estimate of the deviation from this distribution. Given a distribution of states $P(f)$, we can calculate the entropy associated with this distribution of states as

$$S = -\sum_f P(f) \ell n\, P(f) \tag{3}$$

The equilibrium distribution of energy being the most probable thus maximizes the entropy of the system. Any other distribution will result in a lower entropy than that of the prior distribution. However, the most probable distribution is not realized because there are dynamic constraints acting on the colliding particles that move the energy distribution towards a particular direction. The entropy difference $\Delta S = S_{\max} - S$ between these two distributions is

$$\Delta S = \sum_f P(f) \ell n [P(f)/P^0(f)] \tag{4}$$

The actual distribution observed after a chemical reaction could also be defined[1] as the most probable distribution under the physical constraints that apply. In this sense, the actual distribution, being the most probable under the acting constraints, should minimize the entropy difference given by Eq. (4), which will occur when the ratio of the two functions $P(f)/P^0(f)$ becomes maximum. The function $P(f)$ that maximizes this distribution can be given with the aid of Lagrange maximization. This leads us to a series of exponential factors, i.e.,

$$\ell n [P(f)/P^0(f)] = \lambda_0 + \lambda_1 f + \lambda_2 f^2 + \cdots + \lambda_i f^i + \cdots \tag{5}$$

Experimental evidence (a number of examples are given in Ref. 1 and the ones cited therein), has shown that the first-order $f$ is sufficient to describe most postcollision distributions with adequate accuracy.

Combining Eqs. (2) and (5), the energy exchange probability density function therefore takes the form:

$$P(f_a) = \frac{\Gamma(\Xi_a + \Xi_b)}{\Gamma(\Xi_a)\Gamma(\Xi_b)} (f_a)^{\Xi_a - 1}(1 - f_a)^{\Xi_b - 1} \exp(-\lambda_0 - \lambda_1 f_a) \tag{6}$$

In DSMC computations an accept-reject method is used to sample randomly from the distribution $P(f_a)$ to derive the postcollision properties. To do this, the distribution is normalized, eliminating the need to evaluate $\lambda_0$. This leaves us with $\lambda_1$ as the only unknown parameter that has to be determined for each reaction. This can be done by comparison of the theoretical predictions with experimental results, for example, for the reaction rates as shown later in this article. The experimental investigation of Levine and Bernstein[1] indicated that $\lambda_1$ is, in general, a function of the initial and final states of the transition.

For the case of nonreacting flows, the $\lambda_1$ parameter is zero. The model therefore reduces to a conventional Borgnakke and Larsen internal–translational energy exchange as proposed by Bird.[3] In this study a quantized serial application of the generalized Borgnakke–Larsen (B–L) method (see Bird[3]) has been used. For the energy exchange after chemical reactions the same serial application of the method is used, but the exponential term added to the distribution accounts for the effects of nonequilibrium.

For the calculation of the probability of chemical reactions, the principle of microscopic reversibility is used. Using this principle, the ME analysis for the postcollision energy states given in the previous section can be repeated for the reacting energy states to formulate the chemical reaction probabilities. This means that exactly the same formula that was used for the energy disposal [Eq. (6)] of the forward reaction can be used for the prediction of the probability of the reverse chemical reaction. For chemical reaction rates the $\lambda_1$ parameter can been modeled[1,6,7] as a linear function of the reaction energy, i.e., where $\lambda_1 = \lambda_c + \lambda_t T$, where $T$ is the temperature derived from the translational energy of the reacting molecules. Note that when calculating the reaction probability, the $\exp(-\lambda_0)$ factor and the fraction of the gamma functions of Eq. (6) are in effect a steric factor $S$.

The previous analysis for the derivation of the probability distributions shows that with the addition of the exponential term in Eq. (6), effects of nonequilibrium energy exchange can be taken into consideration. It is important to note that the application of the ME method satisfies the principle of microscopic reversibility.

### A. Dissociation Reactions

The dissociation reactions are usually the first ones to take place behind the shock wave in hypersonic flows of a binary mixture of $N_2$ and $O_2$. Dissociation of $O_2$ starts at about 3000 K followed by $N_2$ at about 9000 K. This process being endothermic results in a dramatic degradation of the energy of the flow.

There is broad agreement that for the dissociation reactions of the form $AB + M \rightarrow A + B + M$, the magnitude and mode of excitation of the vibrational energy plays a crucial role in promoting the reaction, provided that the total interaction energy exceeds a threshold. The sensitivity of the reaction probability to the vibrational energy is a function of the total energy available in the collision. The enhancement of endothermic reaction rates has been found[1] to be high for low energies, but as the energy of the reaction increases, the enhancement of the rate is reduced. This behavior can be modeled by the ME method using a $\lambda_1$ parameter that is a decreasing function of the collision energy. As the temperature increases, the actual distribution tends towards the equilibrium one. For exothermic reactions (e.g., recombination reactions) in contrast to endothermic ones, the increase of the rate because of the reagent vibrational energy is lower than expected on prior grounds. It is found that, in accordance with experimental observations, the vibrational energy discourages exothermic reactions from taking place.

In this study the $\lambda_1$ parameters were estimated using a single-cell simulation in which collisions are modeled between equal fractions of the two reagents in an equilibrium state. When collisions occurred, the probability of a reaction taking place was evaluated using the expressions previously stated. After each collision the molecular properties were left unchanged to retain the equilibrium state of the gas. The model parameters were systematically altered until an acceptable agreement with the experimentally measured rates was obtained over the temperature range of interest.

### B. Atom Exchange Reactions

Unlike the dissociation reactions that are controlled by the vibrational energy, measurements of the reaction probability of atom exchange reactions (see Ref. 1) of the form $A + BC \rightarrow AB + C$ indicate that most of these reactions are less sensitive to the vibrational energy of the reagents, and the reaction cross section depends predominantly on the particles' translational energy. An important class of reactions in atmospheric chemistry that presents such a behavior is the exothermic ion–molecule reactions of the form:

$$N^+ + O_2 \rightarrow \begin{cases} NO^+ + O \\ N + O_2^+ \end{cases}$$

This type of reaction is very significant since 28 out of the 68 most common reactions in atmospheric chemistry are exchange reactions. Correct modeling of these reactions is essential since they control the concentrations of the chemical species and they allow low-energy transitions between particles. The two exceptions to this are the two neutral exchange reactions, $NO + O \rightarrow N + O_2$ and $N_2 + O \rightarrow NO + N$, for which there is information that the vibrational energy is the controlling factor.

Equation (6) is symmetric for all energy modes and the $\Xi_a$ term can be replaced with the translational degrees of freedom. The energy exchange for this case is modified accordingly to satisfy the principle of microscopic reversibility. The same linear form for the $\lambda_1$ parameter has been selected. This assumption is arbitrary because virtually no information is available to make a more precise estimation. However, the fitting of the reaction rates to measured data shows that good agreement can be achieved, which gives confidence for the selection of a linear function. A comparison of the ME reaction rate predictions with the experimental data of Park[4] for two exchange reactions is given in Fig. 1. In this example one atom and one ion exchange reaction are included.

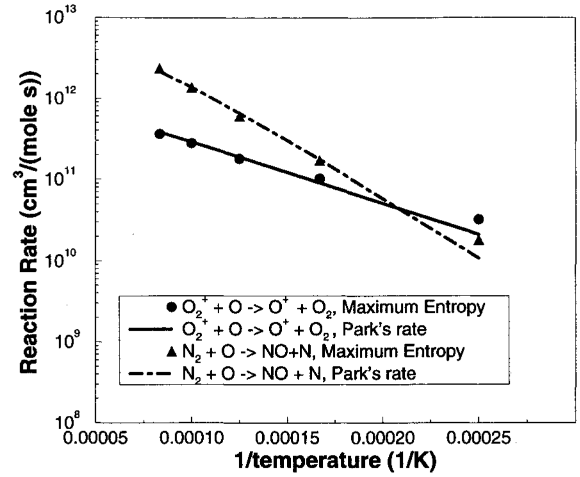

**Fig. 1 Comparison of predicted reaction rates with experimental data.**

The prominent role of the translational energy in these reactions as opposed to the average or the vibrational temperature has been recognized by Park.[4] In this study we will follow Park's model for the exchange reactions.

A list of all the reactions included in this study with their relative controlling mode and the corresponding $\lambda$ parameters and steric factors $S_f$ is given in Table 1.

### C. Interchangeable Energy Modes

Unlike the vibrational energy mode that equilibrates slowly, the rotational mode reaches equilibrium very quickly. The lowest rotational states containing most of this energy are always distributed very closely to the Boltzmann distribution characteristic of the rotational temperature at that point. This temperature may not be the same as the translational temperature during a transient period, but only very few collisions (3–5) per particle are usually enough for the rotational mode to equilibrate closely with the translational mode. As a result, for simulation tests made on isolated gas samples for which energy conservation will apply within the single computational cell, the rotational energy can be assumed to be distributed according to the equilibrium distributions. This limits the nonequilibrium energy exchange to that between the vibrational and the translational mode. The interlinking of these modes poses the question whether within a single-cell equilibrium simulation the vibrational and the translational mode are interchangeable (neglecting electronic excitation), i.e., whether one can discriminate between the effectiveness of either mode in causing a reaction since they are complementary. Satisfactory, but incorrect, results can be produced by single-cell simulations if, for example, the vibrational energy is used to control exchange reactions that in reality are dependent on the translational energy. In a real rarefied hypervelocity flow considerable nonequilibrium between all of the energy modes is the norm, and clearly the correct energy mode that controls the chemical activity for each reaction has to be identified and used in the simulation.

### D. Comparison of the Maximum Entropy with the Equilibrium Methods

There are advantages of using the ME method instead of any of the conventional methods, based directly on the B–L formulation. The ME method recognizes the fact that the energy selectivity of a chemical reaction is followed by energy specificity in the distribution of energy after that collision. In every interaction, energy is distributed in its own way, favoring some energy modes and particular levels. In contrast, the B–L models distribute energy using the same distribution for all interactions, which is physically unrealistic.

When it comes to chemical reactions, the ME method takes into consideration that not all energy states are equally capable of promoting a reaction. With the current modeling the effects

Table 1 ME parameters for chemical reactions

| Reaction | Mode | $S_f$ | $\lambda_c$ | $\lambda_t$ |
|---|---|---|---|---|
| Dissociation reactions | | | | |
| $N_2 + M_2 \rightarrow N + N + M_2$ | $E_{vib}$ | 0.08 | −20 | 0.0003 |
| $O_2 + M_2 \rightarrow O + O + M_2$ | $E_{vib}$ | 1.0 | −27 | 0.0007 |
| $NO + M_2 \rightarrow N + O + M_2$ | $E_{vib}$ | 1.0 | −10 | 0.0003 |
| $N_2 + M \rightarrow N + N + M$ | $E_{vib}$ | 0.2 | −20 | 0.0004 |
| $O_2 + M \rightarrow O + O + M$ | $E_{vib}$ | 1.0 | −10 | 0.0002 |
| $NO + M \rightarrow N + O + M$ | $E_{vib}$ | 1.0 | −10 | 0.0003 |
| $N_2^+ + e^- \rightarrow N + N$ | $E_{trans}$ | 1.0 | −30 | −0.005 |
| $O_2^+ + e^- \rightarrow O + O$ | $E_{trans}$ | 1.0 | −30 | −0.005 |
| $O_2^+ + e^- \rightarrow O + O$ | $E_{trans}$ | 1.0 | −30 | −0.005 |
| Exchange reactions | | | | |
| $NO + O \rightarrow N + O_2$ | $E_{vib}$ | 1.0 | −20 | 0.0004 |
| $O_2 + N \rightarrow NO + O$ | $E_{trans}$ | 0.3 | 10 | −0.0006 |
| $N_2 + O \rightarrow NO + N$ | $E_{vib}$ | 0.8 | −20 | 0.0004 |
| $NO + N \rightarrow N_2 + O$ | $E_{trans}$ | 0.2 | 10 | −0.0001 |
| Ionization reactions | | | | |
| $N + O \rightarrow NO^+ + e^-$ | $E_{trans}$ | 0.003 | 0.0 | 0.0 |
| $N + N \rightarrow N_2^+ + e^-$ | $E_{trans}$ | 0.03 | 0.0 | 0.0 |
| $O + O \rightarrow O_2^+ + e^-$ | $E_{trans}$ | 0.003 | 0.0 | 0.0 |
| $O + e^- \rightarrow O^+ + e^- + e^-$ | $E_{trans}$ | 0.300 | 0.0 | 0.0 |
| $O^+ + e^- \rightarrow O + h\nu$ | $E_{trans}$ | (see Ref. 8) | | |
| $N + e^- \rightarrow N^+ + e^- + e^-$ | $E_{trans}$ | 0.3 | 0.0 | 0.0 |
| $N^+ + e^- \rightarrow N + h\nu$ | $E_{trans}$ | (see Ref. 8) | | |
| Charge exchange reactions | | | | |
| $NO^+ + O \rightarrow N^+ + O_2$ | $E_{trans}$ | 0.006 | 20 | −0.0009 |
| $O_2 + N^+ \rightarrow NO^+ + O$ | $E_{trans}$ | 1.0 | −7 | −0.0006 |
| $N^+ + N_2 \rightarrow N_2^+ + N$ | $E_{trans}$ | 0.4 | 15 | −0.0008 |
| $N + N_2^+ \rightarrow N_2 + N^+$ | $E_{trans}$ | 0.5 | −10 | −0.0001 |
| $N + O_2^+ \rightarrow O_2 + N^+$ | $E_{trans}$ | 0.1 | −20 | −0.0009 |
| $N^+ + O_2 \rightarrow O_2^+ + N$ | $E_{trans}$ | 1.0 | 20 | −0.0006 |
| $O^+ + NO \rightarrow N^+ + O_2$ | $E_{trans}$ | 0.05 | 25 | −0.0009 |
| $N_2 + O_2^+ \rightarrow O_2 + N_2^+$ | $E_{trans}$ | 0.003 | 25 | −0.0003 |
| $O_2 + N_2^+ \rightarrow N_2 + O_2^+$ | $E_{trans}$ | 1.0 | −20 | −0.0008 |
| $O + O_2^+ \rightarrow O^+ + O_2$ | $E_{trans}$ | 0.004 | 15 | −0.0008 |
| $O^+ + O_2 \rightarrow O_2^+ + O$ | $E_{trans}$ | 0.95 | −25 | −0.0008 |
| $NO^+ + N \rightarrow O^+ + N_2$ | $E_{trans}$ | 0.0001 | −40 | −0.0009 |
| $O^+ + N_2 \rightarrow NO^+ + N$ | $E_{trans}$ | 0.2 | 30 | −0.0008 |
| $NO^+ + O_2 \rightarrow NO + O_2^+$ | $E_{trans}$ | 1.0 | 30 | −0.0009 |
| $NO + O_2^+ \rightarrow NO^+ + O_2$ | $E_{trans}$ | 1.0 | −6 | 0.0008 |
| $NO^+ + O \rightarrow O_2^+ + N$ | $E_{trans}$ | 0.1 | 26 | −0.0008 |
| $O_2^+ + N \rightarrow NO^+ + O$ | $E_{trans}$ | 1.0 | 10 | −0.0005 |
| $O^+ + N_2 \rightarrow N_2^+ + O$ | $E_{trans}$ | 0.2 | −30 | −0.0008 |
| $N_2^+ + O \rightarrow O^+ + N_2$ | $E_{trans}$ | 0.2 | −20 | −0.0008 |
| $NO^+ + N \rightarrow N_2^+ + O$ | $E_{trans}$ | 0.1 | 25 | −0.0008 |
| $N_2^+ + O \rightarrow NO^+ + N$ | $E_{trans}$ | 0.2 | −27 | −0.0008 |

of vibrational and translational energy are recognized as independent parameters that can promote a reaction without assuming equilibrium distribution of the energy among all of the possible energy modes.

The inability to predict the nonequilibrium processes using the B–L scheme has led to the introduction of a large number of methods that one way or another use the equilibrium distributions in an attempt to simulate the nonequilibrium processes such as chemical reactions and energy exchange. These methods have been accepted because of their success in predicting the flowfield in the near-equilibrium regime. More specifically, for the prediction of chemical reactions, almost all methods seem to conclude that the reaction probability can be described as

$$P \approx S_f f_i^a (1 - f_i)^b \qquad (7)$$

where $S_f$ is a steric factor [see Eq. (1)], which can be a function of the collision energy, and $f_i$ is the fraction of the total energy in the controlling mode. This mathematical form for the reaction probability has traditionally been used in chemistry. Previous applications[8] used for the estimation of electronic excitation cross sections indicated that appropriate selection of the $a$ and $b$ parameters can simulate almost any cross section.

Cross sections of the form (7) have been used in other applications,[9,10] with the $a$ and $b$ parameters estimated in such a way that the methods predict the same macroscopic reaction rate as that experimentally measured. Although this allows reproduction of the measured reaction rate in equilibrium, coupling these probabilities with the Borgnakke and Larsen energy exchange model leads to violation of the principle of microscopic reversibility (despite the satisfaction of detailed balance), which has to be examined at the individual collision level. Not satisfying the principle of microscopic reversibility means that these methods are unable to establish equilibrium between the forward and reverse reactions at a microscopic level (see Levine and Bernstein[1]), and as a result either the energy exchange or the chemical reaction process (if not both) are in error. Satisfying detailed balance is a necessary, but not sufficient, condition for a method to be microscopically reversible.

In the previous section it was demonstrated that the ME method offers a way to calculate these parameters in a physically realistic way. The ME method includes the effects of nonequilibrium into the exponential factor, which allows the formulation to remain reversible.

### E. Application to Atmospheric Reactions

In this study the set of 68 reactions proposed by Park[4] was adopted. Among these reactions there are 28 that could be identified as atom exchange reactions that can be modeled with the new method. Table 1 gives the reactions that are included in this model with the controlling energy mode. The vibrational mode is $E_{vib}$ and $E_{trans}$ is the translational mode.

Our previous application[7] of the ME method to the calculation of reaction probability of all reactions including the exchange reactions was based solely on the vibrational energy. In Sec. III.C it was noted that in single-cell simulations of reactions, with the gas at equilibrium, the sensitivity of the rate to either the translational or vibrational mode is masked because of the coupling of these two modes in the artificial single-cell simulation. In the present study, modeling of the exchange reactions using the vibrational energy has been replaced with the more accurate translational model.

## IV. Application of the ME Method in DSMC

For energy exchange after chemical reactions controlled by the vibrational mode, the exponential term is added to the vibrational energy distribution, which accounts for the effects of nonequilibrium. The vibrational mode is treated as quantized energy distribution, whereas the rotational and the translational energy modes are treated as continuous energy distributions. In the present study, the anharmonicity of the vibrational states was ignored and the vibrational energy states were assumed to comply to the harmonic oscillator model.

For the calculation of energy exchange the parameters used to obtain the reaction probability of the reverse reaction are used. For simplicity, the temperature dependence of $\lambda_1$ has been ignored and only the $\lambda_c$ parameter is used. For the energy distribution of the dissociation reactions the $\lambda_1$ parameter was estimated to be 8; this value agrees with the observations of Levine and Bernstein[1] for collisional-induced dissociation.

For the treatment of chemical reactions once the total energy of a collision is greater than the reaction energy threshold, the reaction probability is calculated according to the energy in the controlling energy mode. In the case of a successful event, the total energy is distributed to the products with the procedure described at the beginning of this section.

## V. Simulation Results

The new ME model will be compared with the Bird chemistry model for two flowfields. In the first case only neutral species will be treated. In the second example, which is more energetic, the full spectrum of ionic reaction is included. The results of this study have been obtained with an axisymmetric DSMC code employing the variable soft sphere model of Koura and Matsumoto.[11] The code uses structured multiregional meshes, and weighting factors are used to reduce the number of particles required for the simulation. The code simulates the translational, rotational, vibrational, and electronic energy modes. Apart from the vibrational energy modes that are treated in quantum states, all other modes are regarded as having continuous distributions.

Since no reliable experimental results exist for a detailed description of rarefied high enthalpy flowfields, the verification of the new model will be based on comparison with other methods currently available. For this purpose two flow cases will be considered. In the first one the new model will be used for the calculation of the flowfield around the nose area of the Shuttle Orbiter. The same calculation has been performed by Carlson and Bird[12] using Bird's[3] latest model. According to this model the reaction rates are set by the vibrational relaxation and a chemical reaction takes place when the vibrational energy exceeds the dissociation limit. In this model the Borgnakke–Larsen model for inelastic collisions is used to develop closed-form expressions for the reaction rates. The second case simulates the flowfield around the nose area of the Aeroassist Flight Experiment (AFE) vehicle. In this higher enthalpy case the predictions using our new model are compared with those by Gnoffo's LAURA computational fluid dynamics (CFD) code.

### A. Case 1

The nose area of the Shuttle Orbiter was approximated as an axisymmetric flow about a spherically blunted 41.15-deg cone with a tip radius $R = 1.296$ m. The DSMC code makes use of the ME model described in the previous sections. The ambient air conditions were assumed to be those at 92.35 km altitude and the vehicle was flying with a velocity of 7.5 km/s. For the simulation a $60 \times 60$ computational grid was employed. In this study the effect of ionizing reactions has been ignored.

The temperature and density profiles along the stagnation streamline are presented in Fig. 2. In this figure the flow is from right to left and the stagnation point at $x/R = 0$. The translational temperature rises to a peak of about 24,000 K followed by peaks in the rotational (not shown) and the vibrational temperature. The latter peaks at around 9000 K in the shock layer. These temperatures are high enough to provoke chemical reactions in the flow, and since most of these are endothermic, the reaction products are vibrationally cold. The results of this simulation are presented in the figure as closed symbols. The same conditions have been simulated by Carlson and Bird[12] using Bird's latest (1994) chemical reaction model, and the results of their calculation are presented in the same figure as open symbols.

It can be seen that the translational temperatures in both simulations are similar. The striking difference is in the level of the vibrational temperature (11,000 K in the Carlson–Bird calculation). From this figure we note that nowhere in the flow (apart from the surface of the body) was thermal equilibrium achieved.

The mole fractions of the species are presented in Fig. 3. The differences in the vibrational temperature are reflected in the chemical activity of the flow. For the ME prediction the dissociation of $N_2$ starts closer to the stagnation point, although at almost the same vibrational temperature. This indicates that the two models have similar dependence on the vibrational energy for the onset of the dissociation reactions. The minimum concentrations of $N_2$ have been predicted to be the same by both methods, presumably because the flow has reached near-equilibrium conditions by this point. $O_2$ having a smaller energy threshold is less effected by the differences in the temperatures, and the predictions of the two methods are very similar. However, the production of NO within the shock layer is strongly influenced by the different temperatures. Bird's method predicts a higher mole fraction than the ME method by a factor greater than 2. This is to be expected as Bird's method yields higher overall chemical activity because of the higher vibrational temperature.

The prediction of lower vibrational temperatures by the ME method is a significant point that should be noted. Since both methods initiate the chemical reactions at the same vibrational temperature, it is evident that the differences between the mole fractions of $N_2$ and NO have to be a consequence of the different energy exchange processes. The flowfield is dominated by dissociation reactions, and the ME scheme requires that on top of the favorable depletion of the higher vibrational energy states, the products of the dissociation reactions appear vibrationally cold to satisfy detailed balance. The difference between the two models can be expected to become more significant as the flow becomes increasingly rarefied and chemically active.

To study the effects of controlling the exchange reactions with different energy modes, this case was simulated again with all of the exchange reactions controlled by the vibrational mode. In both cases the reaction rates at equilibrium were the same. The temperature profiles along the stagnation streamline are given in Fig. 4. Note that the translational temperature has not been influenced by the different controlling modes. However, significant change can be seen in the vibrational temperatures. The solely vibrationally controlled flowfield exhibited a vibrational temperature about 2000 K greater than for the vibrational–translational controlled flow. As explained in Sec. III.C, at equilibrium one should not be able to see the difference between the two controlling mechanisms. As we move to situations where there is a greater degree of nonequilibrium, the effects of the different energy modes become more significant. The differences in the vibrational temperature result are

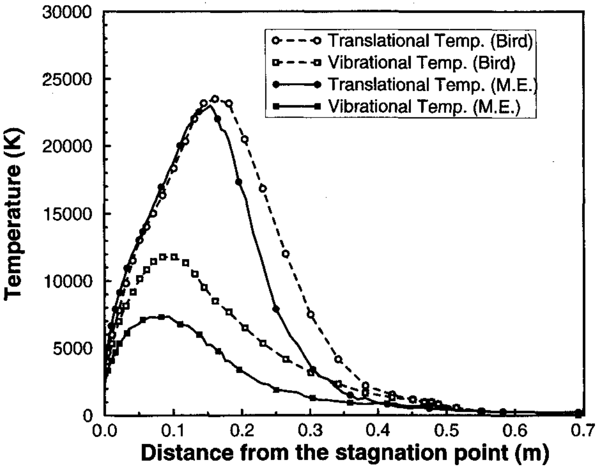

**Fig. 2 Comparison of temperature profile along the stagnation streamline for the Shuttle Orbiter at 92 km.**

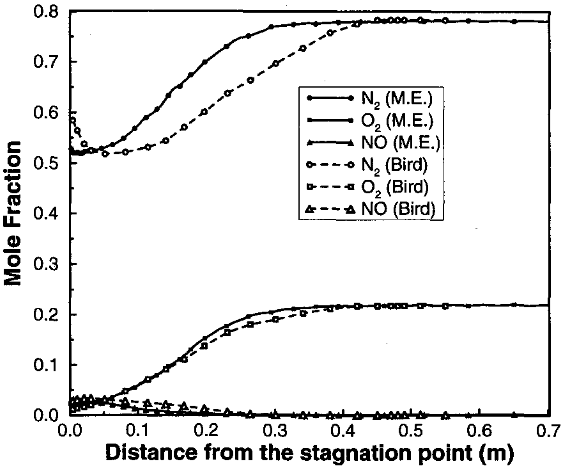

**Fig. 3 Comparison of species mole fractions along the stagnation streamline for the Shuttle Orbiter at 92 km.**

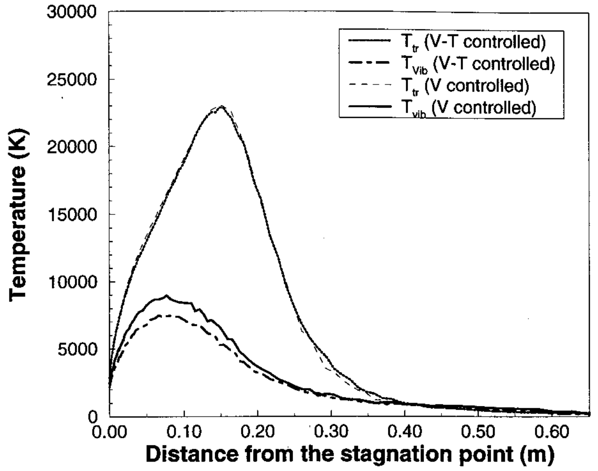

**Fig. 4 Comparison of temperature profile along the stagnation streamline for the Shuttle Orbiter at 92 km for the new and the old ME schemes.**

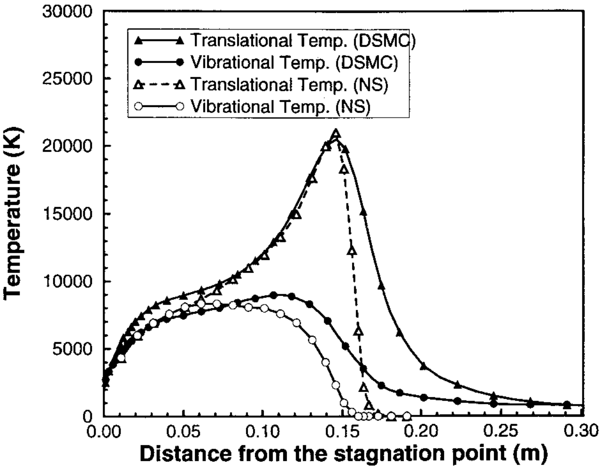

**Fig. 5 Comparison of temperature profile along the stagnation streamline for the AFE at 82.5 km.**

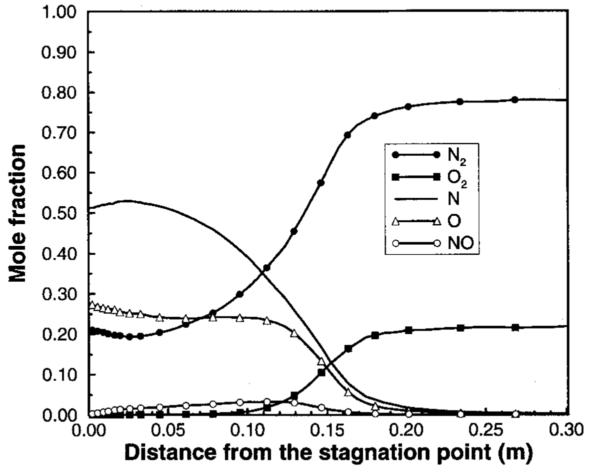

**Fig. 6 Species mole fractions along the stagnation streamline for the AFE at 82.5 km.**

reflected in the mole fraction of NO in the flow. In this example it was found that the new scheme in which two of the exchange reactions were controlled by the translational temperature predicted an NO mole fraction almost double that obtained when all of these reactions were controlled by the vibrational temperature.

### B. Case 2

The second case that was simulated included the effect of the ionic reactions. The flowfield around the AFE was again simulated. For reasons of computational efficiency only the nose region of the AFE was simulated as a sphere with a radius of 2.16 m. The freestream conditions were assumed to be those at 82.53 km attitude. The vehicle was flying at 7.628 km/s. A flow at around 7.5 km/s has enough energy to initiate the 68 most significant chemical and ionic reactions of interest in ($N_2$, $O_2$) air chemistry. As a result of these reactions, the simulated air is a mixture of 11 species, including the electrons. The fact that the energy of the flow is enough to initiate all of the physical processes included in the code makes this case particularly interesting. The conditions of this simulation have been chosen to match those made by Greendyke et al.[13] using the LAURA Navier–Stokes (NS) solver corrected for low-density effects. These continuum calculations used Park's 1987 set of chemical reaction rates, which is slightly different than the one used in our DSMC code that corresponds to Park's 1990 set of data. The LAURA code recognizes as well the dependence of exchange reactions on the translational energy. The vibrational relaxation in the LAURA code was in accordance with the White and Millikan expression, similar to that in the DSMC code, which employs Park's correction for the Millikan and White formula to avoid inappropriately large values of the vibrational relaxation cross section. The LAURA code used Stewart's finite rate catalysis to model the surface chemistry, whereas the DSMC code assumed only recombination between ions and electrons hitting the surface of the vehicle. This difference in the chemical kinetics can be expected to affect the results, but not to a significant degree, since the difference in the reaction rates between the 1987–1990 Park date is not very large. The differences that lie in the fundamental assumption of the two methodologies are more important than the differences in the reaction rates.

Figure 5 shows profiles of temperature along the stagnation line. The flow comes from the right to left. The backscattered particles that diffuse upstream cause the temperature to rise. Ahead of the density shock the translational temperature starts rising at $x = 0.25$ m and reaches a peak of 22,000 K. The vibrational temperature is initiated mainly by the chemical reactions and it starts rising at $x = 0.20$ m. It reaches a peak of 10,000 K behind the peak of the rotational temperature (not shown in this figure). In the same plot the results of the continuum calculation are presented and it can be seen that the translational temperature starts rising at $x = 0.16$ m and then sharply rises to a peak of 22,000 K. The vibrational temperature starts rising almost at the same position, and without a significant peak reaches equilibrium with the translational temperature at $x = 0.05$ m earlier than predicted by the DSMC calculation ($x = 0.02$). Note that the predictions of the two codes are in good agreement in the high-density region close to the body wall where equilibrium conditions apply, while more significant differences appear in the nonequilibrium region. The prediction of larger standoff distances by DSMC codes has been a well-studied effect that has been found in numerous comparisons of DSMC and NS solvers. It is encouraging that the translational and vibrational temperature are, in general, in close agreement. The DSMC codes appear to equilibrate the translational and the vibrational mode later than the NS solver. This is to be expected since in the NS solvers equilibrium distributions are typically used for the calculation of flow properties. The large discrepancy between the DSMC and NS temperature profiles ahead of the shock layer reflects the latter's inability to handle the shock wave in the rarefied upstream flow.

The high temperatures that are met in the flowfield initiate chemical and ionizing reactions. The DSMC prediction for the variation of the chemical synthesis of the flow along the stagnation streamline is shown in Fig. 6. The flow comes from the right to left. At around $x = 0.20$ m, simultaneously with the beginning of the rise of the vibrational temperature, the molecular species start to dissociate. The mole fraction of the atomic species increases until it reaches the ionization area where the rate of increase is reduced. The appearance of the atomic species in the flow is followed by the formation of NO in the area of the shock layer. When the mole fraction of NO has reached its peak value of around 4%, the first electrons appear in the flow. Ionization takes place between the area where the chemical reactions take place and the surface of the body. Electron mole fraction, which equals that of the ionic species, reaches a maximum of 0.9% at $x = 0.053$. The corresponding maximum electron density was found to be $3.0 \times 10^{13}$ $\text{cm}^{-3}$. This value is three times greater than the electron density predicted by the NS solver. Although the DSMC code simulates closely the Park's reaction rates over a range of temperatures, as one can see from Fig. 1, there are some differences that almost certainly contribute to the aforementioned discrepancy.

The temperature standoff distance in the DSMC calculation was found to be greater than the one predicted by the NS solver. This observation is in agreement with numerous previous comparisons between NS and DSMC codes.

## VI. Conclusions

This article presents an extension to a recently introduced maximum entropy collision model (see Gallis and Harvey[2]), which has been developed by the authors for use within the DSMC rarefied flow computational method. The ME formulation recognizes the important role that nonequilibrium effects play in both the initiation of chemical reactions and in the postreaction energy exchange. These effects have long been recognized by chemists, however, the new formulation that uses as a starting point the Borgnakke and Larsen equilibrium distributions, avoids the weakness of the Levine and Bernstein method,[1] which has an implicit assumption of a Maxwell interaction potential. This maximum entropy method has a further advantage over conventional DSMC schemes in that energy is not reassigned after each collision by sampling from an equilibrium distribution, as in the Borgnakke and Larsen formulation. With the new method energy is distributed favoring specific modes and, as a consequence, it is able to satisfy detailed balance unlike other methods being used.

The extension presented here introduces the possibility of reactions that are controlled by the reactants translational energy as opposed to the vibrational energy, which was used for all reactions in our earlier work, but that is responsible for promoting only about two-thirds of the important reactions seen in spacecraft flows in air. Most of the exchange or shuffle reactions are recognized as being controlled by the translational energy, and by modeling this dependence, greater realism is achieved. Note that excellent agreement with the measured reaction rates has now been achieved over a wide range of temperatures for these reactions.

The consequence of the way in which the energy is handled in this new model is that for a typical re-entry vehicle, the flows in the shock layer are vibrationally colder that the Bird model would suggest. This has the effect of slowing down the reactions that are dependent on this energy mode, the most significant being nitrogen dissociation. The move towards using translational energy as the controlling factor for many of the reactions has the effect of changing considerably the mole fractions of the species involved in the exchange reactions, for example, NO.

Comparisons between the new DSMC scheme and Navier–Stokes computations, corrected for low-density effects, show quite sizable differences in the nonequilibrium region, which are not unexpected. Intrinsically, the NS formulation assumes equilibrium distributions within each energy mode as with the Borgnakke and Larsen DSMC scheme.

## References

[1] Levine, R. D., and Bernstein, R. B., *Molecular Reaction Dynamics and Chemical Reactivity*, Oxford Univ. Press, Oxford, England, UK, 1987.

[2] Gallis, M. A., and Harvey, J. K., *The Borgnakke and Larsen Distributions as Prior Distributions in the Maximum Entropy Method, Rarefied Gas Dynamics*, edited by J. K. Harvey and R. G. Lord, Oxford Univ. Press, Oxford, England, UK, 1994.

[3] Bird, G. A., *Molecular Gas Dynamics and the Direct Simulation of Gas Flows*, Clarendon, Oxford, England, UK, 1994.

[4] Park, C., *Non-Equilibrium Aerothermodynamics*, Wiley, New York, 1990.

[5] Haas, B. L., McDonald, L. D., and Dagum, L., "Models of Thermal Relaxation for Particle Simulation Methods," *Journal of Computational Physics*, Vol. 107, No. 2, 1993, pp. 348–358.

[6] Marriott, P. M., and Havey, J. K., "New Approach for Modeling Energy Exchange and Chemical Reactions in the Direct Simulation Monte Carlo Method," *Rarefied Gas Dynamics*, edited by A. E. Beylich and V. C. H. Weinheim, Germany, 1991, pp. 784–791.

[7] Gallis, M. A., and Harvey, J. K., "Application of the Maximum Entropy Method to Energy Exchange, Chemical Reactions and Ionization in the Direct Simulation Monte Carlo Method," Imperial College, AERO Rept. 93-01, London, ISSN 0308-7247, 1993.

[8] Gallis, M. A., and Harvey, J. K., "Atomic Species Radiation from Air Modeled with Direct Simulation Monte Carlo," *Journal of Thermophysics and Heat Transfer*, Vol. 9, No. 3, 1995, pp. 456–463.

[9] Bird, G. A., "Simulation of Multi-Dimensional and Chemically Reacting Flows," *Rarefied Gas Dynamics, 11th Symposium*, edited by R. Campargue, 1979.

[10] Haas, B. L., and Boyd, I. D., "Models for Direct Monte Carlo Simulation of Coupled Vibration Dissociation," *Physics of Fluids A*, Vol. 5, No. 2, 1993, pp. 411–427.

[11] Koura, K., and Matsumoto, H., "Variable Soft Sphere Molecular Model for Inverse-Power-Law or Lenard Jones Potential," *Physics of Fluids A*, Vol. 3, No. 10, 1991, pp. 2459–2465.

[12] Carlson, A. B., and Bird, G. A., "Implementation of a Vibrationally Favoured Dissociation Method in DSMC," *Rarefied Gas Dynamics*, edited by J. K. Harvey and R. G. Lord, Oxford Univ. Press, Oxford, England, UK, 1995, pp. 434–440.

[13] Greendyke, R. B., Gnoffo, P. A., and Wes Lawrence, R., "Calculated Electron Number Density Profiles for the Aeroassisted Flight Experiment," *Journal of Spacecraft and Rockets*, Vol. 29, No. 5, 1992, pp. 621–626.